



## Non-destructive Corrosion Monitoring of Reinforced Concrete Steel Rebars in Chloride Media by Smartphone Magnetic and Analog Hall-Effect Sensors

B. Hazrati Dorigh<sup>a</sup>, E. Khakzadeh<sup>b</sup>, I. Ahadzadeh\*<sup>b</sup>, R. Salamat-Ahanghari<sup>a</sup>

<sup>a</sup> Department of Chemistry, Faculty of Basic Sciences, Azarbaijan Shahid Madani University, Tabriz, Iran

<sup>b</sup> Department of Physical Chemistry, Faculty of Chemistry, University of Tabriz, Tabriz, Iran

### PAPER INFO

#### Paper history:

Received 24 May 2023

Received in revised form 21 June 2023

Accepted 29 June 2023

#### Keywords:

Concrete Corrosion

Corrosion Monitoring

Electromagnetic Sensor

Hall-Effect Sensor

Smart Phone

LCR Meter

### ABSTRACT

The corrosion of reinforced concrete (RC) is a leading cause of structural failures and engineering problems in current infrastructural aspects; making corrosion monitoring of reinforcements in concrete structures highly important especially from safety point of view. Non-destructive testing (NDT) methods are useful approaches for in-situ detection and evaluation of steel corrosion in RC for monitoring time trend of corrosion of rebars. Recently, some NDT methods such as magnetic and resistive sensors as well as electrochemical monitoring methods such as electrochemical impedance spectroscopy were developed for RC rebar corrosion monitoring. This paper presents a novel approach using modern smartphones equipped with magnetic sensors and commercially available analog Hall-Effect sensors to monitor rebar corrosion within the concrete. Results showed a reasonable sensitivity of the methods to detect and monitor corrosion of rebars with time. In order to check and validate the data obtained in this study, another non-destructive electromagnetic test by a search coil connected to a LCR meter was used to monitor corrosion. The results obtained with this method were consistent with the previous methods. In other words, by using these three methods, it is possible to successfully monitor and determine the severity of corrosion.

doi: 10.5829/ije.2023.36.09c.06

## 1. INTRODUCTION

To increase the strength of concrete structures, many strategies have been adopted, among these methods is the use of concrete reinforced with rebars, but due to the presence of corrosive species in the environment, the problem of corrosion of rebars has become a global challenge, so these rebars are being continuously inspected and monitored for corrosion [1]. The environment species that cause most of the corrosion of rebars inside structures include chloride, sulfide and carbon dioxide ions, which facilitate the corrosion of the structure with oxygen and some of the negative effects of chloride infiltration into concrete are as follows:

a) It destroys the passive layer of the steel rebar and makes possible the corrosion attack.

b) By reducing the solubility of  $\text{Ca}(\text{OH})_2$ , it causes the pH of infiltrated water to decrease.

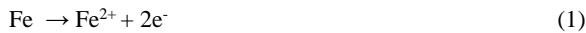
c) Due to the hygroscopic property of salts in concrete (such as  $\text{NaCl}$ ,  $\text{CaCl}_2$ ), it increases the amount of humidity, and d) It increases the electrical conductivity of the concrete [2].

Common methods of reducing corrosion damage of reinforced concrete include correct selection of metal, proper design, cathodic protection, anodic protection, coating and corrosion inhibitors [3].

The whole corrosion process in concrete rebar can be expressed as depicted in Figure 1.

Corrosion of steel in concrete is a result of the dissolution of iron in pore water, which can be indicated as anodic and cathodic reactions mentioned in Equations (1)-(5). At the anodic site, the reaction of Equation (1) occurs:

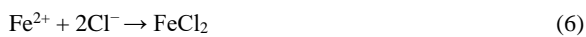
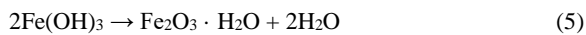
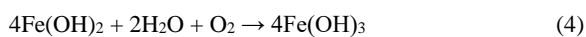
\*Corresponding Author Email: [ahadzadeh@tabrizu.ac.ir](mailto:ahadzadeh@tabrizu.ac.ir)  
(I. Ahadzadeh)



In the cathode site, due to the presence of  $\text{O}_2$  and  $\text{H}_2\text{O}$  ions, the cathodic reaction is expressed in the form of Equation (2):



If the attacking ions are not present in the pore solution, the reactions of Equations (3)-(5) continue to occur, but in the presence of ions such as chlorine, the reaction of Equation (6) is performed, which prevents the formation of a passive layer on the surface of the rebar [4].



Corrosion of steel bars embedded in reinforced concrete structures reduces the useful life and durability of structures causing premature failure of the structure, which has a significant cost for the inspection and maintenance of the structures that are being destroyed. Therefore, monitoring the corrosion of reinforcements is very important to prevent the premature failure of structures [5-8]. Recently, different methods have been implemented to monitor corrosion in reinforced concrete structures. They are classified into six main categories as follows:

Visual Inspection, Electrochemical Methods, Electromagnetic (EM) Waves, Infrared Thermography (IRT), Optical Sensing Methods, and Elastic Wave Method. Each of these 6 methods is classified into various corrosion monitoring methods. For example, among the various techniques for monitoring corrosion

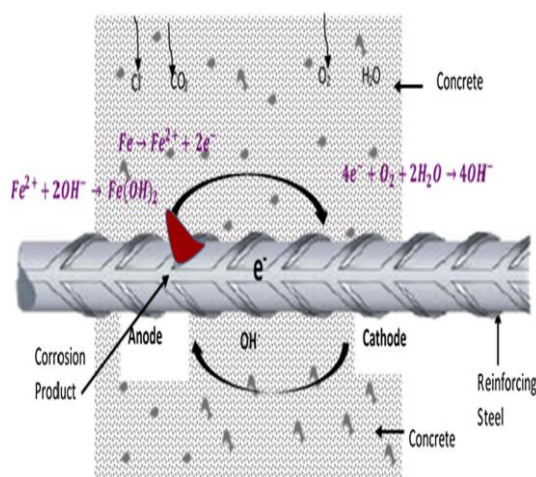


Figure 1. Schematic of corrosion concrete rebar [8]

by electrochemical method, the open circuit potential technique, resistance method, polarization resistance, galvanostatic pulse method (GPM), electrochemical noise (EN), impedance (EIS), and Tafel could be mentioned [9]. Each of these methods has its own disadvantages and advantages. However, it is almost impossible to identify and locate corrosion damage with solely electrochemical devices [10]. Nowadays, monitoring devices such as electromagnetic sensors, acoustic emission analyzers, X-ray machines, industrial CTs, optical fiber sensors, and digital imaging techniques have emerged based on various physical fields. Among these devices, first electromagnetic sensors and then digital image technology are considered as the best methods for monitoring the corrosion of steel buried in reinforced concrete and the deformation of concrete surface [11].

Nowadays, smartphone has become an important tool for corrosion monitoring. The sensors in the smartphone have been used to collect data for processing and evaluation and final explanation [6, 12]. Hall-Effect sensor is one of the types of electromagnetic sensors. The Hall-Effect sensor is a device that is activated by applying a magnetic field. Magnetic flux density intensity and polarity (north and south poles) are two important characteristics of the magnetic field. When the magnetic flux density around the sensor exceeds a certain threshold, the sensor recognizes this issue and produces an output voltage called "Hall voltage". Recently, smartphones have been equipped with a feature in sensors such as magnetic sensors, acceleration sensors, pressure, temperature sensors. Smartphones equipped with a magnetic sensor can be used as a detector to measure the magnetic field [13, 14]. The innovative aspect of this research is the monitoring of steel corrosion in reinforced concrete using the electromagnetic method by the smartphone equipped with the Hall effect sensor.

Zhang et al. [13] have used an innovative magnetic-based corrosion evaluation apparatus to investigate the fundamental relationship between corrosion rate and magnetic induction surrounding steel reinforcement. This apparatus can be embedded directly inside reinforced concrete structures and monitor the rate of corrosion of the reinforcement. The preliminary calibration results show that there is a linear relationship between the weight loss of corrosive reinforcement with the voltage increment detected by the Hall-effect sensor surrounding the corroded reinforcement. This increment in voltage is due to the variation of magnetic field induction [13]. Zhang et al. [15] have presented a non-destructive method for monitoring steel corrosion in reinforced concrete bridges by using a 3D digital micromagnetic sensor. In their research, the setup of the magnetic scanning device and the measurement mode of the micromagnetic sensor have been examined to detect and analyze the leakage of the magnetic field from corroded

reinforced concrete. On the other hand, the numerical analysis model has also been developed and presented based on the linear magnetic charge theory. By comparing magnetic field leakage data and numerical calculations, the authors have concluded that the tangential magnetic field curves cross at different heights near the corrosion zone. As a result, through the intersection of magnetic field curves, it is possible to detect and evaluate the steel corrosion area in reinforced concrete [15]. Li et al. [11] have introduced a novel electro-magnetic monitoring apparatus (EMMA) to monitor the corrosion of reinforced bars in concrete. Novel EMMA has twenty-four Hall-effect sensors embedded and a magnification monitoring probe that can detect variations in the intensity of the magnetic field of reinforced bars in concrete. As their results showed, the magnetic flux varied with the occurrence of corrosion, and this variation increased the Hall-effect voltage at cross-section of the reinforced concrete [11]. Van Steen et al. [16] have used the acoustic emission (AE) technique to monitor corrosion. Results show that AE can detect damage during the corrosion process [16]. Elyasigorji et al. [17] have introduced a DC magnetic field in the vicinity of the reinforcing steel in concrete to detect the corrosion of the prestressing steel of the magnetic flux leakage (MFL) concept in several configurations. The results indicate that the variations in the induced magnetic field are due to the presence of corrosion [17].

The LCR meter method is another modern corrosion monitoring method. The basis of this method is based on the change of parameters L (inductance), C (capacitance), R (resistance) and Q (quality factor) of an electric circuit element applied as sensor. In common researches, the coil is used as a monitoring probe in series with the LCR meter device, and when corrosion occurs, the values of L and Q change according to the amount of corrosion [18].

In this research, a simple and non-destructive method of smartphone and Hall effect sensor methods were used to monitor corrosion. Results were obtained regarding the location of corrosion, intensity and depth of corrosion, and mechanism of corrosion.

## 2. EXPERIMENTAL

To monitor the corrosion of reinforced concrete, a simulation of industrial structures was used. The smartphone's magnetic sensor and analog Hall-Effect sensor was used to corrosion monitoring and the LCR meter was used to monitor and validate the obtained data.

**2.1. Materials** A plastic cast with a length of 22.7 cm, a width of 14.9 cm, and a height of 4.9 cm was used to make a reinforced concrete block (Figure 2) [19-22].

The mixing ratio of Portland cement and sand is 1:5. Four rebars were used with a length of 140 mm and a diameter of 8 mm, and the position of the rebars is 40 mm apart and 10 mm deep in the concrete [23-25].

**2.2. Methodology** In order to monitor the corrosion of reinforced concrete with a smartphone and Hall-Effect sensor, first the rebars in the concrete have been made to undergo intentional accelerated corrosion. Considering that the corrosion of steel is basically a time-consuming process, it is possible to induce the corrosion of the reinforced concrete steel sample by applying direct

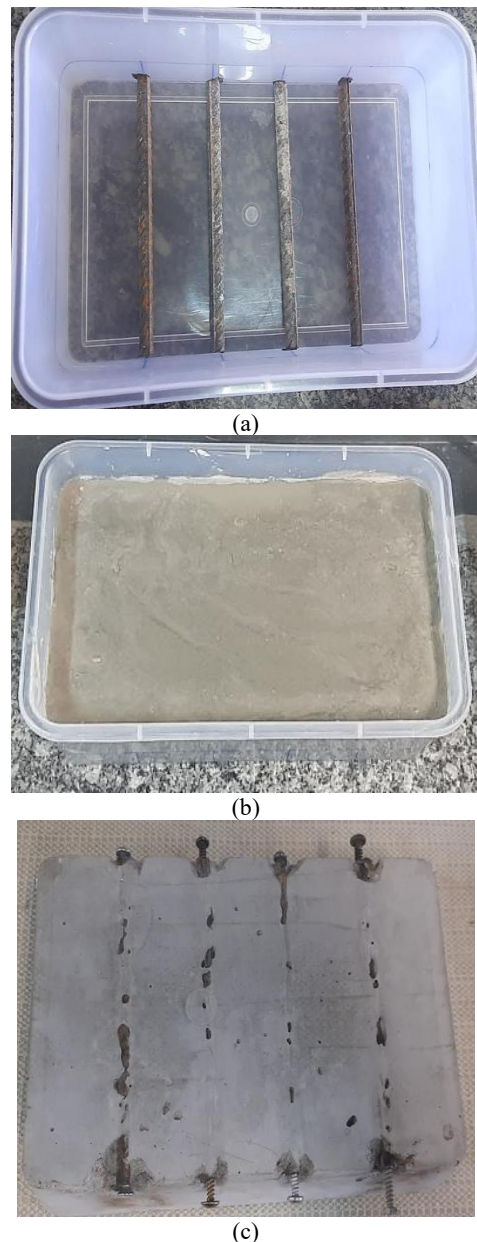


**Figure 2.** Schematic of steps for preparation of concrete block



current to the steel rebars in contact with a chloride electrolyte. Humidity, temperature, current density, carbon concentration, chlorine concentration, cement content, types of cement, etc. are important factors in the design of an intentional acceleration corrosion test method. The applied current density is known to be an essential parameter for intentionally accelerated corrosion [26]. The schematic of the corrosion process setup is shown in Figure 3. In this research, the applied potential between the cathode and the anode (rebar) is about 30 V by the help of an ADAK PS405 power supply (Iran) to start the corrosion of three rebars, which in the long time causes corrosion of the target rebars and corrosion products cause micro-cracks in the concrete.

According to Figure 4, the areas marked with hatches are the location of the stainless steel cathode on the sponge dipped in salt water, and these points are subject to selective corrosion. Area number 1 (rebar number 2) for 12 hours, area number 2 (rebar number 3) for 14 hours, and area number 3 (rebar number 4) for 10 hours have been subjected to a constant voltage of 30 volts.

After the intentional acceleration of corrosion, at first, a smartphone equipped with a magnetic sensor was employed to monitor the corrosion. The magnetic sensor in Samsung A30s series smartphones is activated by installing the Engineering Toolbox Application. The calibration of magnetic corrosion monitoring devices was necessary before the use of this device to detect corrosion of reinforced concrete structures. The calibration process is performed with the aim of increasing the voltage of the sensor. As shown in Figure 5, a smartphone was used for corrosion monitoring based on a non-destructive (electromagnetic) way.

As shown in Figure 6, a ratiometric linear analog Hall-Effect sensor (OMH3150) was used for corrosion monitoring based on a non-destructive (electromagnetic) method. The output of this sensor is 2.5 volts in the absence of a magnetic field due to the application of 5 volts and when the sensor is placed on the S pole side of the structure, the output voltage value of this sensor increases and when it is placed on the N pole side of the structure, the voltage value. The output of this sensor decreases and finally the voltage changes are proportional to the changes in the intensity of the magnetic field. As the Hall-Effect sensor was moved in different areas of the reinforced concrete surface, the analog output voltage changed.

Finally, according to Figure 7, the LCR meter device (UNI-T(UT,612), China) was used to verify the data obtained. This technique involves the combination of a search coil (about 11 mm in diameter, 25 turns of 0.3 mm copper wire) and a LCR meter device at fixed frequency of 100 kHz. By moving the search coil on the surface of the concrete in regular pattern for corrosion monitoring, the LCR meter device indicates the inductance ( $L$  in  $\mu\text{H}$ ) and quality factor of the inductor ( $Q$ , as a dimensionless

number). Finally, it can be concluded that this simple experimental setup employing a search coil can easily be used for monitoring corrosion through recording spatial changes of  $L$  and  $Q$  parameters by an LCR meter. As the

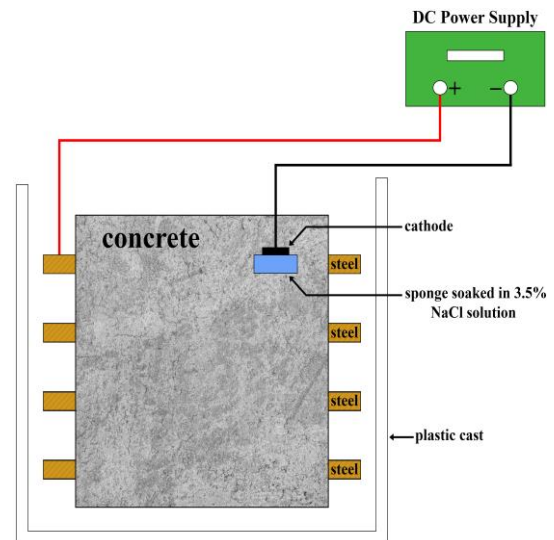


Figure 3. The schematic of the corrosion process setup

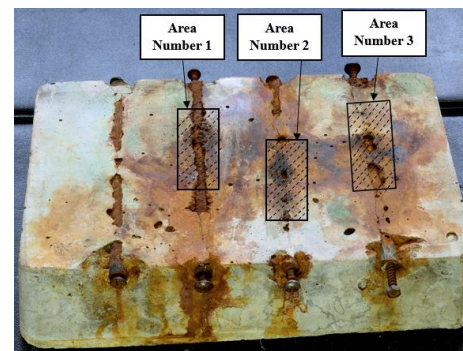


Figure 4. View of the reinforced concrete after intentional corrosion

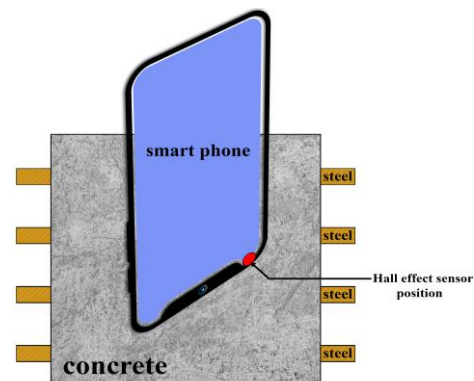


Figure 5. Schematic of corrosion monitoring of rebars in reinforced concrete by a smartphone equipped with a Hall-Effect sensor

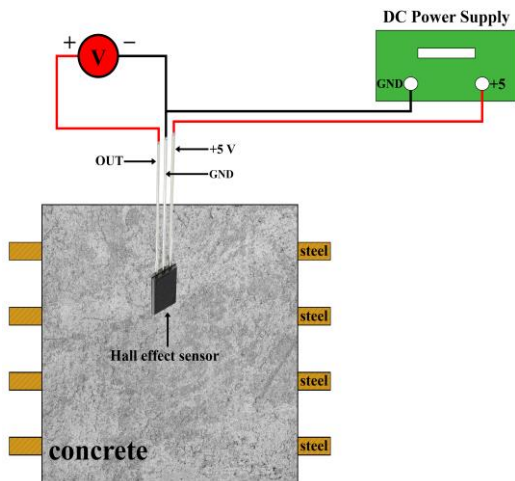


Figure 6. Schematic of corrosion monitoring of rebars in reinforced concrete by an analog Hall-Effect sensor



Figure 7. Schematics of corrosion monitoring of rebars in reinforced concrete by a LCR meter

coil moves on the reinforced concrete surface, the L and Q values change. According to Equation (7), at a frequency of 100 kHz, one can obtain the resistance R (in Ohms) from the relationship between Q (dimensionless number) and L (in  $\mu\text{H}$ ):

$$R = \frac{(0.628 \times L)}{Q} \tag{7}$$

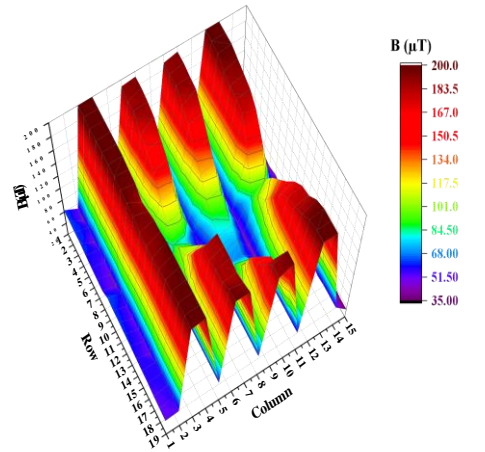
### 3. RESULTS AND DISCUSSIONS

#### 3. 1. Corrosion Monitoring with a Smartphone Magnetic Sensor

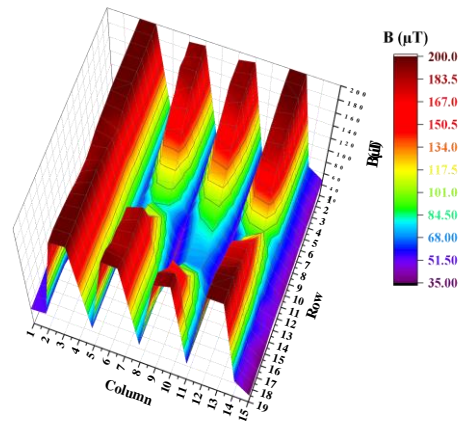
Figure 8 shows the three-dimensional plot of the magnetic field signals measured by the smartphone on concrete and four rebars that had limited corrosion. By analyzing the sensor signals, it is possible to check the corrosion progress of reinforced concrete steel bars.

According to Figure 8, the areas with the highest magnetic field (139.1-200  $\mu\text{T}$ ) were not corroded. The

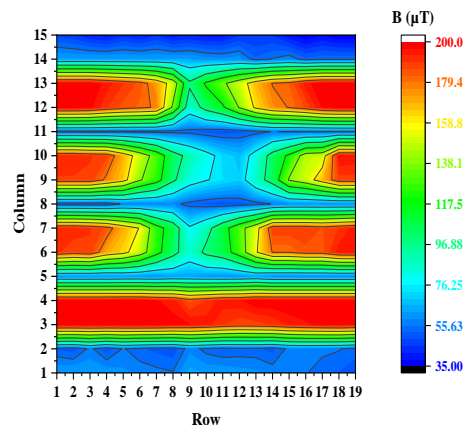
areas with a magnetic field (96.88-139.1  $\mu\text{T}$ ) detect rebars that have suffered from partial corrosion. The



(a)



(b)



(c)

Figure 8. (a), (b) The 3D-Colormap and (c) the Contour-Color Fill plots of corrosion monitoring by a smartphone, i.e. magnetic field intensity ( $\mu\text{T}$ ) at various point of the surfaced concrete block

rebars showing a relatively low magnetic field (55.63-96.88  $\mu\text{T}$ ) have suffered from relatively severe corrosion. Concrete itself has a magnetic field of 35-55.63  $\mu\text{T}$ . As a result, rebar 2 is corroded at distances 6 and 7 on the Y-axis (column) and between distances 4 and 14 on the X-axis (row). Rebar 3 is corroded at distances 9 and 10 on the Y-axis (column) and between distances 4 and 14 on the X-axis (row). Rebar 4 is corroded at distances 12 and 13 on the Y-axis, and between distances 6 and 14 on the X-axis. Therefore, the areas drawn in dark blue color represent the intact concrete areas; the areas drawn in light blue color indicate the part where the rebar has been corroded, and the areas drawn in red, orange, and yellow color indicate the areas in which the rebar, in comparison to the areas with light blue, has the greatest magnetic field and is not affected by corrosion.

As shown in Figure 9, the magnetic field of the corroded rebars is between the magnetic field of the non-corroded rebar and concrete. Rebar 1 has the highest magnetic field because it has not been affected by intentional corrosion. Therefore, rebar 2 is more corroded than rebar 4, and rebar 3 is more corroded than rebars 2 and 4. Rebar 3 has the longest length of corrosion. The Hall-Effect sensor is used in corrosion science to detect the metallic properties of metals and the areas of the rebar that have corroded. Therefore, the output signals from the Hall-Effect sensor in the areas with a low magnetic field indicate the area of concrete. By detecting and analyzing the output signals using a smartphone, we find that the magnetic field intensity plots all intersect at the same point and the distance between the intersection points can be used as a measure of the length of the corrosion area.

### 3. 2. Corrosion Monitoring by a Hall-Effect Sensor

Figure 10 shows the three-dimensional plot of the

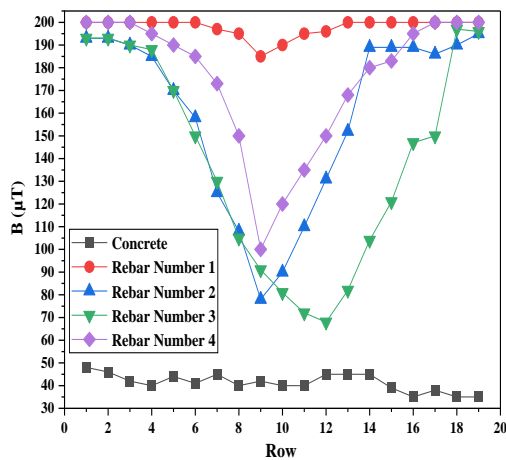


**Figure 9.** Profile of the concrete block, corroded rebars, and non corroded rebar by a smartphone equipped with a Hall-Effect sensor, i.e. magnetic field intensity ( $\mu\text{T}$ )

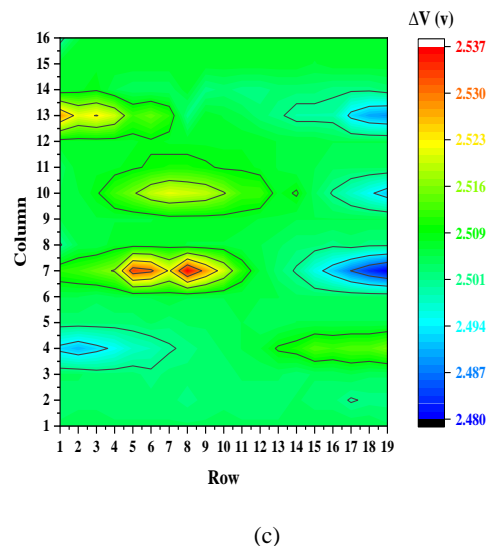
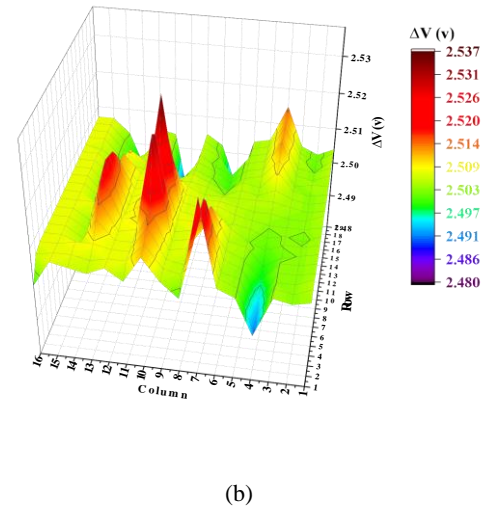
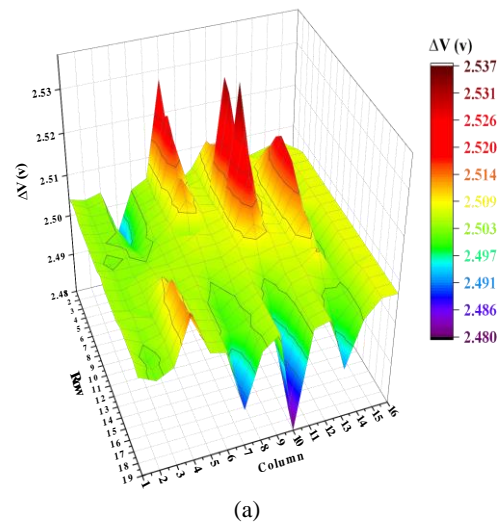


**Figure 10.** (a), (b) The 3D-Colormap and (c) the Contour-Color Fill plots of corrosion monitoring by a Hall-Effect sensor, potential difference (voltage) at various point of the surfaced concrete block



magnetic field signals as recorded by a Hall-Effect sensor on concrete and four rebars.

According to Figure 10, Rebar 2 has been corroded between distances 6 and 7 on the Y-axis (column) and between distances 1 to 3, 6 to 8 and 16 to 19 on the X-axis (row). Rebar 3 has been corroded between distances 9 and 10 on the Y-axis (column) and between distances 6 to 8, and 8 to 19 on the X-axis. Rebar 4 has been corroded between distances 12 and 13 on the Y-axis (column) and between distances 10 to 13 and 14 to 19 on the X-axis. During smartphone monitoring, the corroded areas in Rebar 2 were detected at distances 7 and 12, in Rebar 3 at distances 6 and 17, and in Rebar 4 between distances 8 to 13 on the X-axis. When the Hall-effect sensor moves from one side of the rebar to the other, the potential difference changes, with the highest and lowest values indicating the peak and valley areas, respectively, as shown in Figure 10 (a and b). The areas shown in green represent the concrete itself and a part of the rebar embedded in the concrete at a lower depth. The areas drawn with red, orange, and yellow colors, respectively indicate the areas with the greatest potential difference. The areas drawn with red, orange, and yellow colors, respectively represent the areas that have the greatest potential difference, and the areas drawn with blue color represent the areas of the rebar that may be corroded. According to these statements, it can be concluded that rebar 1 is not corroded and only in the first rows it may suffer minor corrosion.

Figure 11 shows that by detecting and analyzing the voltage output signals from the Hall-effect sensor, the potential difference of a part of the corroded rebar is between the potential difference of the concrete and that of the non-corroded rebar. Therefore, rebar 3 has the lowest potential difference and has the longest corrosion rate, in agreement with corrosion monitoring results using a smartphone. On the other hand, in rebars 2, 3 and 4, the potential difference is much less in the last rows (16-19) than in the first rows (1-5) due to rebar displacement. Because the rebar 1 may be affected by the corrosion products of other corroded rebars, the potential difference in this rebar is almost small in the first rows compared to the last rows. By comparing Figures 9 and 11, for corrosion monitoring with a smartphone and Hall-Effect sensor, respectively, the magnetic field and potential difference as output signals for corroded rebar are in midway of their corresponding values for concrete and corrosion-free rebar, and rebar number 3 has the lowest magnetic field and potential difference. Because rebar number three has been affected by intentional corrosion for more hours than rebar number two and four, through corrosion monitoring using these two methods, it can be seen that rebar number three has been corroded more and the length of the corrosion zone is long in this rebar.

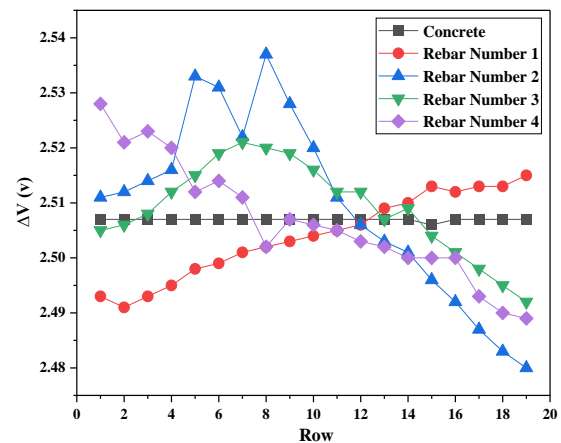


**Figure 11.** Profile of the concrete block, corroded rebars, and non corroded rebar by a Hall-Effect sensor, potential difference (voltage)

In general, according to the graphs drawn, through corrosion monitoring using these two methods, the corrosion locations can easily be visually identified. The time evolution of corrosion can also be studied. It is possible to select areas with a certain corrosion rate based on the intensity of the field changes and to monitor corrosion without the need to destroy concrete or apply external current to the reinforcement bars, especially in complex structures. Finally, larger diameter rebars can be monitored at greater depth.

**3. 3. Corrosion Monitoring by a LCR Meter** In order to validate the data obtained from the previous two methods, the LCR meter was used and the results are reported in Figure 1Y. According to Equation (7), the higher the corrosion rate of the rebar, the more the behavior of the coil moves towards being ideal and the Q factor increases and the R-value decreases. Therefore, in areas where the amount of Q increases, it indicates more corrosion of the rebar in that area.

According to the diagrams in Figure 12, the X-axis is row, the Y-axis indicates column and the Z-axis shows R. Rebar 2 is corroded at a distance of 6 in the Y axis (column) and between distances 1.5 to 3 in the X axis (row). Rebar 3 is corroded at distance 9 in the Y axis (column) and between distances 2.5 and 4 in the X axis. Rebar 4 is corroded at a distance of 12 in the Y axis (column) and between 1.5 and 3 in the X axis. The areas drawn with red, orange and yellow colors, respectively represent the areas that have the highest resistance, and the areas drawn with light blue and green colors represent the areas of rebar that are corroded and have the lowest resistance value. In areas where the value of R has decreased, it indicates local corrosion in that area. The results are completely consistent with the two previous methods and confirm the previous results.

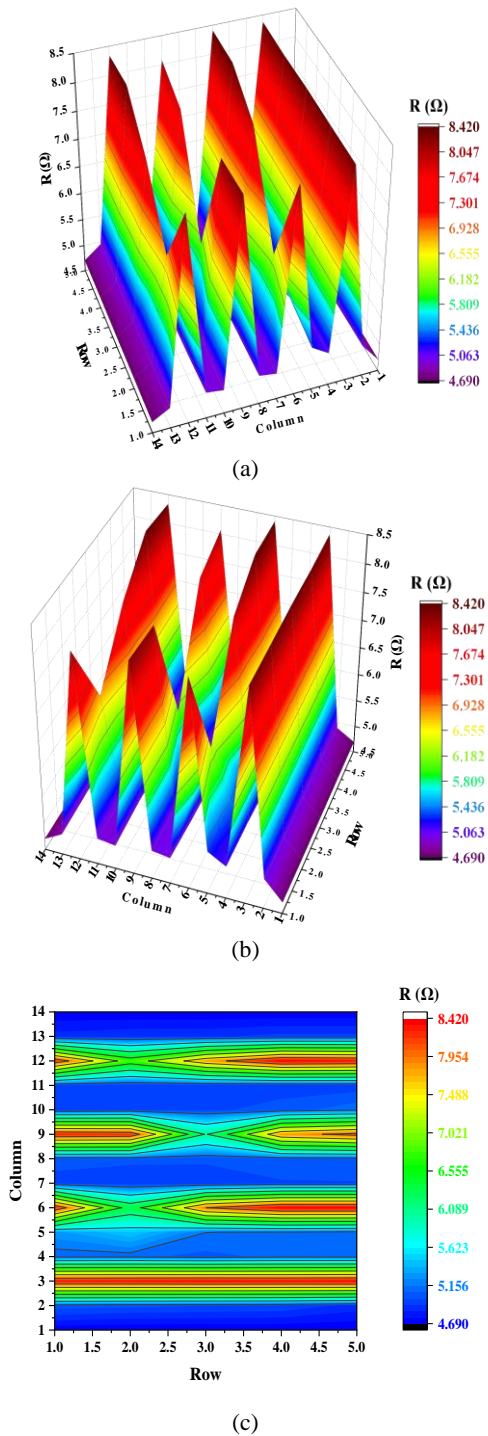


**Figure 12.** (a), (b) The 3D-Colormap and (c) the Contour-Color Fill plots of corrosion monitoring by a LCR coil sensor

As shown in Figure 13, by detecting and analyzing the output signals from the search coil, the strength value of corroded rebars is between the strength of non-corroded rebar and concrete. Rebar 1 has the highest

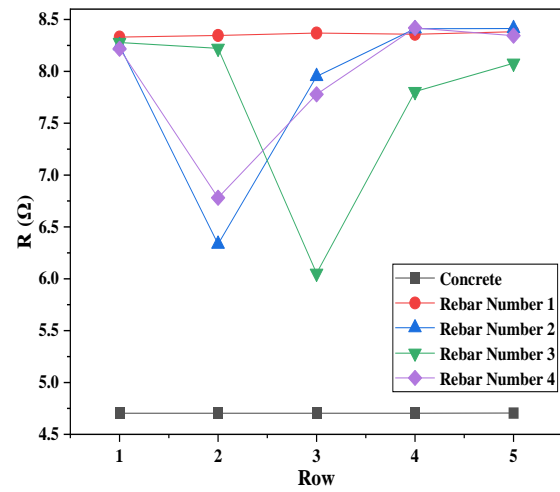


**Figure 13.** Profile of the concrete block, corroded rebars, and non corroded rebar by a LCR meter, resistance (Ω)

resistance value because it has not been affected by intentional corrosion. Rebar 2 is corroded more than rebar 4, and rebar 3 is corroded more than rebar 2 and 4, which is due to the difference in the duration of selective corrosion.

#### 4. CONCLUSIONS

In this research, two new cost-effective electromagnetic methods were developed to monitor the corrosion of reinforced concrete and the results were compared and verified with the LCR method. The main conclusions are as follows:

1. When the corrosion occurred, the intensity of the induced magnetic field increases of Hall-Effect voltage at the cross-section of reinforced concrete.
2. A smartphone is capable of detecting as well as monitoring corrosion initiation and location of the reinforcement bars inside concrete based on the electromagnetic properties of the corroded reinforced bars.
3. The results of corrosion monitoring by a smartphone and the Hall effect sensor are in agreement with LCR meter and therefore, the smartphone and Hall-effect sensor can be used for monitoring purposes due to ease of operation, small size, and low cost.
4. The advantages of these methods are non-destructiveness, simplicity of use, short test duration, being inexpensive compared to other methods, precise determination of the depth and area of the rebar under corrosion, precise determination of the location of the cut rebar, and to some extent determining the corrosion mechanisms that can be determined by the time evolution of corrosion data.



## 5. REFERENCES

- Sikarwar, S., Singh, S. and Yadav, B. C., "Review on pressure sensors for structural health monitoring", *Photonic Sensors*, Vol. 7, (2017), 294-304. doi: 10.1007/s13320-017-0419-z.
- Fanijo, E. O. and Brand, A. S., "Anti-corrosion behaviors of corn-based polyols on low carbon steel rebar", *Cleaner Materials*, Vol. 4, (2022), 100066. doi: 10.1016/j.clema.2022.100066.
- Broomfield, J. P., "Corrosion of steel in concrete: understanding, investigation and repair", *CRC Press*, (2023). doi: 10.1201/9781003223016.
- Goyal, A., Pouya, H. S., Ganjian, E. and Claisse, P., "A review of corrosion and protection of steel in concrete", *Arabian Journal for Science and Engineering*, Vol. 43, (2018), 5035-5055. doi: 10.1007/s13369-018-3303-2.
- Daniyal, M. and Akhtar, S., "Corrosion assessment and control techniques for reinforced concrete structures: a review", *Journal of Building Pathology and Rehabilitation*, Vol. 5, (2020), 1-20. doi: 10.1007/s41024-019-0067-3.
- Safaie, N., Hamidi, H. and Vali, M., "A Framework for Analysis of Predictors of Mobile-marketing Use by Expanding Unified Theory of Acceptance and Use of Technology and Artificial Neural Networks", *International Journal of Engineering, Transactions B: Applications*, Vol. 36, No. 05, (2023), 1012-1022. doi: 10.5829/IJE.2023.36.05B.17.
- Shadmand, M., Hedayatnasab, A. and Kohnehpooshi, O., "Strengthening of rc beams using steel plate-fiber concrete composite jackets (finite element simulation and experimental investigation)", *International Journal of Engineering, Transactions A: Basics*, Vol. 35, No. 1, (2022), 73-92. doi: 10.5829/IJE.2022.35.01A.07.
- Quraishi, M., Nayak, D., Kumar, R. and Kumar, V., "Corrosion of reinforced steel in concrete and its control: An overview", *Journal of Steel Structures & Construction*, Vol. 3, No. 1, (2017), 1-6. doi: 10.4172/2472-0437.1000124.
- Azarsa, P. and Gupta, R., "Electrical resistivity of concrete for durability evaluation: a review", *Advances in Materials Science and Engineering*, (2017). doi: 10.1155/2017/8453095.
- Li, Z., Jin, Z., Shao, S. and Xu, X., "Magnetic properties of reinforcement and corrosion products described by an upgraded monitoring apparatus", in Proceedings of the 7th World Conference on Structural Control and Monitoring, Qingdao, China., 1397, (2018).
- Li, Z., Jin, Z., Gao, Y., Zhao, T., Wang, P. and Li, Z., "Coupled application of innovative electromagnetic sensors and digital image correlation technique to monitor corrosion process of reinforced bars in concrete", *Cement and Concrete Composites*, Vol. 113, (2020), 103730. doi: 10.1016/j.cemconcomp.2020.103730.
- Taspika, M., Nuraeni, L., Suhendra, D. and Iskandar, F., "Using a smartphone's magnetic sensor in a low-cost experiment to study the magnetic field due to Helmholtz and anti-Helmholtz coil", *Physics Education*, Vol. 54, No. 1, (2018), 015023. doi: 10.1088/1361-6552/aaefb4.
- Zhang, J., Liu, C., Sun, M. and Li, Z., "An innovative corrosion evaluation technique for reinforced concrete structures using magnetic sensors", *Construction and Building Materials*, Vol. 135, (2017), 68-75. doi: 10.1016/j.conbuildmat.2016.12.157.
- Akimitsu, M., Ono, Y., Cao, Q. and Tanabe, H., "High-Resolution 2D Magnetic Field Measurement of Magnetic Reconnection Using Printed-Circuit Board Coils", *Plasma and Fusion Research*, Vol. 13, (2018), 1202108-1202108. doi: 10.1585/pfr.13.1202108.
- Zhang, H., Liao, L., Zhao, R., Zhou, J., Yang, M. and Xia, R., "The non-destructive test of steel corrosion in reinforced concrete bridges using a micro-magnetic sensor", *Sensors*, Vol. 16, No. 9, (2016), 1439. doi: 10.3390/s16091439.
- Van Steen, C., Verstrynghe, E., Wevers, M. and Vandewalle, L., (2019). "Assessing the bond behaviour of corroded smooth and ribbed rebars with acoustic emission monitoring", *Cement and Concrete Research*, Vol. 120, (2019), 176-186. doi: 10.1016/j.cemconres.2019.03.023.
- Elyasigorji, A., Rezaee, M. and Ghorbanpoor, A., "Magnetic corrosion detection in concrete structures", In International Conference on Sustainable Infrastructure 2019, Leading Resilient Communities through the 21st Century. Reston, VA: American Society of Civil Engineers., (1398), (2019).
- Ha, N., Lee, H. S., and Lee, S., "Development of a Wireless Corrosion Detection System for Steel-Framed Structures Using Pulsed Eddy Currents", *Sensors*, Vol. 21, No. 24, (2021), 8199. doi: 10.3390/s21248199.
- Sivamani, J., Thiyaneswaranb, M. and Navaneethanb, K. S., "Performance Studies on Glass Fiber Reinforced Recycled Aggregate Concrete", *International Journal of Engineering, Transactions B: Applications*, Vol. 36, No. 05, (2023), 904-913. doi: 10.5829/IJE.2023.36.05B.07.
- Mohammadi, Y. and Asilb, M. B., "Utilization of Steel Micro-fiber and Carbon Nanotubes in Self-compacting Lightweight Concrete", *International Journal of Engineering, Transactions B: Applications*, Vol. 36, No. 5, (2023), 955-964. doi: 10.5829/IJE.2023.36.05B.15.
- Pawar, A. J., Patel, M. and Suryawanshi, S. R., "Finite Element Modelling of Laboratory Tests on Reinforced Concrete Beams Containing Recycled Aggregate Concrete", *International Journal of Engineering, Transactions B: Applications*, Vol. 36, No. 5, (2023), 991-999. doi: 10.5829/IJE.2023.36.05B.15.
- Masne, N. and Suryawanshi, S., "Effect of replacement ratio on torsional behaviour of recycled aggregate concrete beams", *International Journal of Engineering, Transactions A: Basics*, Vol. 36, No. 4, (2023), 659-668. doi: 10.5829/IJE.2023.36.04A.06.
- Tumengkol, H., Irmawaty, R., Parung, H. and Amiruddin, A., "Precast Concrete Column Beam Connection Using Dowels Due to Cyclic Load", *International Journal of Engineering, Transactions A: Basics*, Vol. 35, No. 1, (2022), 102-111. doi: 10.5829/IJE.2022.35.01A.09.
- Sijwal, G., Pradhan, P. and Phuvoravan, K., "Lateral Load Carrying Capacity of Concrete-filled Cold-formed Steel Shear Wall", *International Journal of Engineering, Transactions A: Basics*, Vol. 35, No. 1, (2022), 161-171. doi: 10.5829/IJE.2022.35.01A.15.
- Dhundasi, A., Khadirnaikar, R. and Momin, A. I. A., "Stress-strain characteristics of reactive powder concrete under cyclic loading", *International Journal of Engineering, Transactions A: Basics*, Vol. 35, No. 1, (2022), 172-183. doi: 10.5829/IJE.2022.35.01A.16.
- Feng, W., Dong, Z., Liu, W., Cui, H., Tang, W. and Xing, F., "An experimental study on the influence of applied voltage on current efficiency of rebars with a modified accelerated corrosion test", *Cement and Concrete Composites*, Vol. 122, (2021), 104120. doi: 10.1016/j.cemconcomp.2021.104120.

**COPYRIGHTS**

©2023 The author(s). This is an open access article distributed under the terms of the Creative Commons Attribution (CC BY 4.0), which permits unrestricted use, distribution, and reproduction in any medium, as long as the original authors and source are cited. No permission is required from the authors or the publishers.



---

**Persian Abstract**

---

**چکیده**

خوردگی بتن مسلح (RC) یکی از دلایل اصلی خرابی سازه و مشکلات مهندسی در جنبه‌های زیر ساختی است که سبب اهمیت پایش خوردگی آرماتورها در سازه‌های بتنی به‌ویژه از نظر ایمنی می‌شود. روش‌های آزمایش غیرمخرب (NDT)، رویکردهای مفیدی جهت تشخیص و ارزیابی لحظه‌ای خوردگی فولاد در RC برای پایش با روند زمانی خوردگی میلگردها هستند. اخیراً برخی از روش‌های NDT مانند سنسورهای مغناطیسی و مقاومتی و همچنین روش‌های پایش الکتروشیمیایی مانند طیف‌سنجی امپدانس برای پایش خوردگی میلگرد در RC توسعه داده شده‌اند. این مقاله رویکرد جدیدی را با استفاده از تلفن‌های هوشمند مدرن مجهز به حسگرهای مغناطیسی و حسگرهای آنالوگ اثر هال موجود، برای پایش خوردگی میلگرد در بتن ارائه می‌کند. نتایج حاکی از حساسیت معقول روش‌های تشخیص و پایش خوردگی میلگردها با گذشت زمان برخوردار می‌باشد. در این تحقیق، دو روش توسعه‌یافته شده، مناسب، امکان‌پذیر و مقرون به صرفه هستند و می‌توانند برای نظارت میدانی قوی میلگردها در مهندسی عمران استفاده شوند. به منظور بررسی و اعتبارسنجی داده‌های به‌دست‌آمده در این پژوهش، از آزمایش غیر مخرب الکترومغناطیسی دیگری توسط یک سیم پیچ جست‌وجوی متصل به یک LCR متر برای نظارت بر خوردگی استفاده شد. نتایج به دست آمده با این روش با روش‌های قبلی مطابقت داشت. به عبارت دیگر، با استفاده از این سه روش می‌توان با موفقیت پایش و شدت خوردگی را تعیین کرد.

---